Energy Beamforming for Cooperative Localization in Wireless Powered Communication Network

Yubin Zhao, *Member, IEEE,* Xiaofan Li, *Senior Member, IEEE,* Huaming Wu, *Member, IEEE,* and Cheng-Zhong Xu, *Fellow, IEEE*

***Abstract*—Two functions are essential and necessary for wireless powered communication network, which are energy beamforming and localization. On one hand, energy beamforming controls the wireless energy waves of energy access point (E-AP) in order to activate the nodes for transmitting information. On the other hand, locating the nodes is important to network management and location based services in WPCN. For large scale network, cooperative localization which employs neighborhood nodes to participate in positioning unknown target nodes is highly accurate and efficient. However, how to use energy beamforming to achieve high accurate localization is not fully investigated yet. In this paper, we analyze the impacts of energy beamforming on the cooperative localization performance of WPCNs. We formulate the Fisher information matrix (FIM) and the corresponding Cramér-Rao lower bound (CRLB) for the full connected network and a single node respectively. Then we propose beamforming schemes to optimize the cooperative localization and the power consumption. For optimal localization problems, we derive the close-form expression of the optimal energy beamforming. And for the optimal energy efficiency problems, we propose semi-definite programming (SDP) solutions to achieve the minimum power consumption while using calibrations to approach the actual localization requirements. Further, we also analyze the impacts of channel uncertainty. Through extensive simulations, the results demonstrate the dominant factors of the localization performance, and the performance improvements of our proposed schemes, which outperform the existing power allocation schemes.**

***Index Terms*—wireless power transfer, cooperative localization, Fisher information matrix, semi-definite programming, energy efficiency**

I. Introduction

In the recent years, radio frequency (RF) power transfer has become effective alternative technique to supply continuous energy for the remote next-generation wireless networks [1]. The conventional energy constrained wireless networks have a limited lifetime, which consume lots of efforts to maintain the batteries, such as wireless sensor networks. In contrast, the wireless network equipped with RF energy harvesting module has a sustainable power supply from radio environment. Consequently, with the appearing of the commercialized products, e.g., Powercast, wireless power communication networks (WPCNs) have drawn much attention [2]. As a promising network of future IoT systems, the architecture, waveform design, beamforming and network optimization are extensively investigated.

Compare with wireless communication networks (WCNs) [3], WPCNs show advantages in lifetime and cost. The lifetime of WPCN can be extended as long as possible with a single energy access point (E-AP). Because such E-AP can provide continuously wireless energy for the passive nodes. The lifetime of WCN is limited by the batteries equipped in the nodes. No matter what kind of energy efficient strategies are used, the batteries will be depleted finally. Even if all the nodes are connected with the power lines, the mobility is limited and the costs are increased. In addition, the cost of each node in WPCN is much lower than WCN, since no battery is required and the architecture of the chip is much simpler. In this case, large-scale network can be constructed.

Similar to other wireless networks, WPCNs contain a large number of deployed nodes sensing, gathering and communicating information with other nodes [4]. Therefore, the knowledge of node positions is becoming important for network management and optimization strategies. On the other hand, positioning the nodes in WPCNs also provides cost effective location based services. However, using GPS is not only an expensive solution but infeasible in some harsh environments, e.g., in buildings, in urban canyons, under tree canopies or in caves. Thus, a fast, cost-effective and high accurate localization technique is required for large scale WPCNs.

Cooperative localization employs nodes exchange radio signals to attain the range measurements [5]. Such technique offers additional localization accuracy gain by enabling the neighbor nodes to help each other in estimating positions, which is suitable for WPCNs in a high density and large scale deployment scenario. In cooperative localizations, nodes with known positions are called anchors, which are sparsely deployed and used to locate other nodes. The nodes with unknown positions are called targets. In WPCN, all nodes including anchors and targets are batteryless and powered up by the E-APs, which are either centralized deployed with MIMO antennas or distributed deployed throughout the playing field. The ranging measurements of cooperative localization can be

Yubin Zhao is with the School of Microelectronics Science and Technology, Sun Yat-Sen University, Zhuhai, 519082, China. Email: zhaoyb23@mail.sysu.edu.cn

Xiaofan Li is the corresponding author who is with the School of Intelligent System Science and Engineering, Jinan Unniversity, Zhuhai, 519070, China. Email: lixiaofan@jnu.edu.cn

Huaming Wu is with the Center for Applied Mathematics, Tianjin University, Tianjin, 300072, China. Email: whming@tju.edu.cn

Cheng-Zhong Xu is with State Key Lab of IoTSC & Dept. of Computer and Information Science, University of Macau, Macau, 999078, China; Email: czxu@um.edu.mo

This work was partially supported by National Key R&D Program of China (No. 2019YFB2102100), National Nature Science Foundation of China (No. 61801306), Shenzhen Fundamental Research (No. JCYJ20180302145755311), Guangdong Special Fund for Science and Technology Development (No. 2019A050503001), Science and Technology Development Fund of Macao S.A.R (FDCT) under number 0015/2019/AKP.

attained only as if the nodes gain enough energy from E-APs. Thus, the microwave propagations in cooperative localization based WPCN consist of energy beamforming of E-AP and the rangning measurements. And the energy beamforming directly influences the ranging and the localization accuracy [6], [7]. Using the cooperative localization technique, the WPCN has two kinds of potential applications. On one hand, WPCN can track nodes widely deployed in the environment without considering the battery depletion, e.g., the sensor tags in manufactory, hospital and tunnel [8], [9]. In addition, the UAVs are potential mobile wireless power transfer devices for such application [10]. On the other hand, such system can be used as the indoor localization for large scale shop malls or factories, since the battery-less nodes can be designed as anchors, which are activated by the wireless power. Such devices are small and the cost is even small than other indoor localization systems, e.g., iBeacon [11].

To analyze the impact of energy beamforming on localization performance in this paper, the Fisher information matrix (FIM) is utilized as the fundamental tool and squared position error bound (SPEB) is introduced as the major metric for evaluation, which are widely applied in many researches [12]–[14]. Within the FIM framework, the beamed wireless power signal, channel information, network topology are fully analyzed, and the optimization objectives are constructed. Then, wireless power beamforming strategies can be developed to minimize the position estimation errors or the energy consumption.

Our major contributions are as follows: Firstly, we formulate the FIM of full-connected WPCN within a cooperative framework, which fully considers the energy beamforming, network topology, signal noise and cooperative ranging measurements. The impacts of beamforming waves on localization performance in E-APs are clearly illustrated in the form of the FIM. Then, the second contribution is that we introduce the beamforming schemes to solve two optimization problems, which are the minimization of position estimation error with transmitted power constraints and the minimization of energy consumption problem with node localization requirements. We prove that the SPEBs in the objectives are bounded by the inverse forms of the FIM trace, in which the objectives are turned into quadratically constraint quadratic programmings (QCQPs). Then, the optimization problems are efficiently solved by obtaining the close form expression or using semi-definite programming (SDP). Thirdly, the spatial recursive FIM formulations and optimization strategies for a single node are exploited with the prior information of other nodes. We derive the upper bound of spatial recursive FIM to develop simplified beamforming solutions. To overcome the over relaxation problems, we employ a calibration method for the SDP solutions. The final contribution is that we analyze the impacts of channel estimation error on localization estimation performances.

Our analysis and proposed beamforming schemes are evaluated in extensive simulations. We compare our schemes with SDP based power allocation solutions and equally combing method. Then, the impacts considering the channel uncertainty are also presented. The results demonstrate that our schemes can greatly improve the estimation accuracy and reduce the minimum energy consumption with a given localization requirement.

The rest parts of this paper are organized as follows: Sec. II presents the related works of the WPCN and cooperative localization; Sec. III provides the system model and the FIM formulations; the beamforming schemes for full connected network are introduced in Sec. IV and the optimizations for single node are presented in Sec. V; Sec VI formulates the impacts of channel uncertainty; the simulations are presented in Sec. VII and Sec. VIII concludes the whole paper.

II. Related Work

WPCN has gain much attention since it is firstly introduced in [15], [16]. Then, many researches utilize various techniques to improve the data transmission quality or reliability, e.g., beamforming strategies [17], [18], network design [19], [20], MAC control schemes [21], [22], cooperative strategies [23], [24]. Considering 3D space, UAVs are employed as the wireless power transfer base stations, and the related joint resource allocation and trajectory plan are investigated [10], [25]. Recently, some passive devices in WPCN are designed to provide localization services, e.g., using backscatter communications [26] or converting the harvested energy into UWB signals [27]. Pannuto et al. proposed a UWB based backscatter device which can achieve 30 cm localization accuracy [28]. Fantuzzi et al. proposed circuit designs to convert the UHF microwave into UWB signals and provide TDOA ranging [29]–[31].

In addition to hardware design, communication strategies and localization methods in WPCNs are also exploited, especially in WSN area. El et al. proposed a hop count method to estimate the node positions in energy harvested WSN [32]. Chang et al. introduced a passive WSN, in which the node was activated by the RF power, and angle division and grid division methods were developed with adapting the RF propagation directions to derive the node positions [33]. Belo et al. used an antenna array to estimate single node location based on RSS value [34]. Aziz et al. introduced a batteryless IoT node with two antennas, and employed 64 antenna array to simultaneously provide wireless power and track the node [35]. In [36], the batteryless anchors are introduced and power allocation schemes for single target tracking are proposed to improve the system performance. Although some localization algorithms are investigated in WPCN, these methods are only applicable for single node or target, which is difficult to implement in large scale network.

In wireless cooperative localization researches, lots of theoretical investigations and localization algorithms appear in the recent years [37]. In general, cooperative localization is an efficient method of self-organized large-scale network to manage the network and tracking multiple targets. However, the localization error can also propagate throughout the whole network when the target nodes contain localization errors and help locate the new joined node. Shen et al. derived the equivalent Fisher information matrix (EFIM) of cooperative localization and used squared position error bound (SPEB) as the main metric to evaluate the positioning accuracy [38]. This work demonstrated that lots of targets provide ranging information when only a few anchors are deployed in a large scale

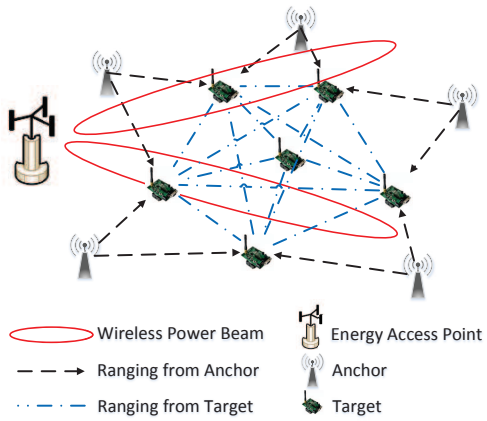

Fig. 1. The architecture of WPCLoc.

network. Then, the localization accuracy is increased with such information. However analyzing the fundamental performance of cooperative localization is complex. Consequently, resource allocations are also complex and the distributed strategies may only converge to local optimal values. Thus, the power control and bandwidth allocation schemes using SDP, gaming and machine learning methods for wideband systems are exploited [39]–[42]. For cooperative localization algorithms, distributed localization algorithm outperforms the centralized algorithm in cooperative localization since the data flow from targets and anchors are reduced. In this case, the operation expense of cooperative localization is much lower than the conventional localization. A linear distributed algorithm framework is introduced in [43]. Nguyen proposed a least squared method in the cooperative localization [44]. Further, semi-definite programming for relaxing the least squared method was also proposed in [45]. Note that, compared with WCNs, the localization accuracy of WPCN is lower with the same number of nodes. Because, the power transfer efficiency of WPCN is quite low, which leads to the low accuracy estimation. In addition, the nodes of WPCN are also low power chips, which means that the nodes can only provide single frequency carrier RSS value for ranging. However, nodes in WCN are active which can provide wide-band singles for localization, e.g., CSI values. In this case, the accuracy is much higher than WPCN. However, the theoretical foundations and optimizations for cooperative localization in WPCNs are not fully investigated yet.

III. System Model

The WPCN consists of E-AP and the wireless communication nodes, which is illustrated in Fig. 1. The nodes with perfect knowledge of their positions are defined as anchors, and the nodes without their position knowledge are defined as targets. All the nodes are equipped without batteries. We use N_A and N_T to denote the number of anchors and targets respectively. The set of anchors is denoted by $\mathcal{N}_A = \{1, 2, \ldots, N_A\}$ and the set of targets is denoted by $\mathcal{N}_T = \{1, 2, \ldots, N_T\}$. The position of anchor j is denoted by $\mathbf{a}_j \triangleq [a_j^X, a_j^Y]^T$, and the position of target i is denoted by $\mathbf{p}_i \triangleq [p_i^X, p_i^Y]^T$.

The E-AP contains multiple antennas and provides the wireless power beam to turn on the batteryless nodes. We use K to denote the number of antennas in E-AP. Let $\mathbf{G} \triangleq [\mathbf{g}_1, \mathbf{g}_2, \ldots, \mathbf{g}_N]^T$ be the downlink wireless power channel matrix from the E-AP to the nodes, and define $g_{kn} \triangleq [\mathbf{G}]_{kn}$ as the channel coefficient between the k-th antenna of the E-AP and the node n. To distinguish the wireless power beam channel to the anchors and the cooperative nodes, we define $\mathbf{G}_A$ as the anchor channel matrix which indicate the channel from E-AP to the anchors, and define $\mathbf{G}_C$ as the target channel matrix to indicate the channel from E-AP to the target nodes. Let $d_{ji} = ||\mathbf{a}_j - \mathbf{p}_i||$ be the range (or distance) between anchor j and target i. Similarly, let $d_{im} = ||\mathbf{p}_i - \mathbf{p}_m||$ be the range between target i and m, where $i \neq m$. The anchors will send ranging signals to the targets when attaining sufficient energy, and the targets also send the ranging signals to each other to form a full connected network and cooperatively locate themselves.

A. Wireless Power Transfer Phase

The E-AP generates a signal vector $\boldsymbol{x} = [x_1, x_2, \ldots, x_K]^T$ to form a wireless power beam. The anchors are activated by such signals. On the network node side, the received signal for node n is:

$$y_n = \mathbf{g}_n \boldsymbol{x} + v_0^n = \sum_{k=1}^{K} g_{kn} x_k + v_0^n \tag{1}$$

where $n \in \mathcal{N}_A \bigcup \mathcal{N}_T$ and v_0^n is the additive noise which follows zero-mean Gaussian distribution. For the wireless power beam, we assume that the received energy is mainly from the E-AP, and v_0^n is too small to power up the device, which can not be collected as the energy source. Then, the received power $r_y^n = \mathbb{E}_{y_n}(||y_n||^2)$ of the node n is:

$$r_y^n = \mathbb{E}_{\boldsymbol{x}}(\boldsymbol{x}^T \mathbf{g}_n^T \mathbf{g}_n \boldsymbol{x}) \tag{2}$$

B. Cooperative Range Measurement Phase

After obtaining the energy from E-AP, network nodes, including anchors and targets, will encode the ranging data and forward to the other nodes. When node n sends the ranging signal to target i, the received signal is:

$$z_{ni} = h_{n,i}(d_{n,i}) y_n + v_e^{ni} \tag{3}$$

where $n \neq i$, $h_{n,i}(\cdot)$ is the channel response of y_n which considers the path loss according to the range $d_{n,i} = ||\boldsymbol{p}_n - \boldsymbol{p}_i||$ between node n and i. Take a flat fading propagation channel for instance, we have $h_{ni}(d_{n,i}) = (\frac{f_c}{4\pi d_{n,i}})^{\beta} \sqrt{\xi_{n,i}}$ where f_c is the central frequency of the signal, β is the fading factor, and $\xi_{n,i}$ is the channel gain.

C. Fisher Information Matrix

To derive the fundamental performance, we employ FIM as the analysis tool. Firstly, we define $\boldsymbol{\theta}$ as the vector of the unknown target position states:

$$\boldsymbol{\theta} = [\mathbf{p}_1^T \ \mathbf{p}_2^T \ \ldots \ \mathbf{p}_{N_T}^T]^T \tag{4}$$

Then, we define $\boldsymbol{z}$ as the observation vector of all the received signals on the target side:

$$\boldsymbol{z} = [\boldsymbol{z}_A^T \ \boldsymbol{z}_C^T]^T \tag{5}$$

where $\boldsymbol{z}_A$ and $\boldsymbol{z}_C$ indicate the observations from anchors and cooperative targets respectively:

$$\begin{cases} \boldsymbol{z}_A = [\boldsymbol{z}_1^{A^T} \ \boldsymbol{z}_2^{A^T} \ \dots \ \boldsymbol{z}_i^{A^T} \ \dots \ \boldsymbol{z}_{N_T}^{A \ T}]^T \\ \boldsymbol{z}_C = [\boldsymbol{z}_1^{C^T} \ \boldsymbol{z}_2^{C^T} \ \dots \ \boldsymbol{z}_i^{C^T} \ \dots \ \boldsymbol{z}_{N_T}^{C \ T}]^T \end{cases} \tag{6}$$

and $\boldsymbol{z}_i^A$ and $\boldsymbol{z}_i^C$ indicate the received signal vectors of target i from anchors and targets respectively:

$$\begin{cases} \boldsymbol{z}_i^A = [z_{1i} \ z_{2i} \ \dots \ z_{ji} \ \dots \ z_{N_A i}]^T \\ \boldsymbol{z}_i^C = [z_{1i} \ z_{2i} \ \dots \ z_{mi} \ \dots \ z_{N_T i}]^T \end{cases} \tag{7}$$

where $m \in \mathcal{N}_T$. Here we define $z_{ii} = 0, i \in \mathcal{N}_T$ for future calculation. The joint probability distribution $f(\boldsymbol{\theta}, \boldsymbol{z}) = f(\boldsymbol{z}|\boldsymbol{\theta})f(\boldsymbol{\theta})$, where $f(\boldsymbol{z}|\boldsymbol{\theta})$ is the likelihood function, and $f(\boldsymbol{\theta})$ is the prior distribution of $\boldsymbol{\theta}$. And, $f(\boldsymbol{z}|\boldsymbol{\theta})$ can be expressed as:

$$f(\boldsymbol{z}|\boldsymbol{\theta}) = \prod_{i=1}^{N_T}(\prod_{m=1}^{N_T} f(z_{mi}|\boldsymbol{p}_i) \prod_{j=1}^{N_A} f(z_{ji}|\boldsymbol{p}_i)) \tag{8}$$

where we define $f(z_{ii}|\boldsymbol{p}_i) = 1, i \in \mathcal{N}_T$.

Next, we define $\widetilde{\boldsymbol{\theta}}$ as the unbiased estimator of $\boldsymbol{\theta}$ based on $\boldsymbol{z}$. The CRLB indicates that the covariance of $\widetilde{\boldsymbol{\theta}}$ should satisfy the information inequality:

$$\mathbb{E}_{\boldsymbol{z},\boldsymbol{\theta}}\{(\widetilde{\boldsymbol{\theta}} - \boldsymbol{\theta})(\widetilde{\boldsymbol{\theta}} - \boldsymbol{\theta})^T\} \succeq \mathbf{J}_{\boldsymbol{\theta}}^{-1} \tag{9}$$

where $\mathbf{J}_{\boldsymbol{\theta}}$ is the FIM for $\boldsymbol{\theta}$ given by:

$$\mathbf{J}_{\boldsymbol{\theta}} = \mathbb{E}_{\boldsymbol{z},\boldsymbol{\theta}}\{\nabla_{\boldsymbol{\theta}} \ln f(\boldsymbol{\theta}, \boldsymbol{z})[\nabla_{\boldsymbol{\theta}} \ln f(\boldsymbol{\theta}, \boldsymbol{z})]^T\} \tag{10}$$

where $\nabla_{\boldsymbol{\theta}}$ is the first order partial derivatives operator of $\boldsymbol{\theta}$. Then, we have the following proposition.

Proposition 1. *The FIM of all the target nodes in WPCN is given by (12) on top of the next page where $\mathbf{J}_{\boldsymbol{\theta}}$ is a $2N_T \times 2N_T$ matrix. And $\mathbf{J}_A(\boldsymbol{p}_i)$ and $\mathbf{C}_{i,m}$ are expressed as follows:*

$$\begin{cases} \mathbf{J}_A(\boldsymbol{p}_i) = \sum_{j=1}^{N_A} \lambda_{j,i}\mathbf{J}(\phi_{j,i}) & j \in \mathcal{N}_A \\ \mathbf{C}_{m,i} = (\lambda_{i,m} + \lambda_{m,i})\mathbf{J}(\phi_{m,i}) & i, m \in \mathcal{N}_T \end{cases} \tag{11}$$

where $\lambda_{m,i}$ is derived based on (47); $\mathbf{J}(\phi_{m,i}) = \mathbf{q}_{m,i}\mathbf{q}_{m,i}^T$ is the angle-of-arrival (AOA) matrix, $\mathbf{q}_{m,i} = [\cos\phi_{m,i} \ \sin\phi_{m,i}]^T$ with $\phi_{m,i} = \arctan\frac{p_i^X - p_m^X}{p_i^Y - p_m^Y}$ denoting the AOA from the node m to the node i.

Proof. *Refer to Appendix A for the detailed derivation.*

Note that, this FIM formulation is constructed based on the framework of cooperative localization [38]. Proposition 1 illustrates the relationship between the wireless power transfer and the localization accuracy and provides the new model of equivalent ranging coefficient (ERC) within the FIM framework. Specifically, $\lambda_{i,m}$ and $\lambda_{j,i}$ are re-formulated compared with [38], where $\lambda_{i,m}$ is formulated as:

$$\lambda_{i,m} = r_y^m \frac{\xi_{i,m}\beta^2(\frac{f_c}{4\pi})^{2\beta}}{d_{i,m}^{2\beta+2}N_0} \tag{13}$$

in which r_y^m is determined by the wireless node since the node is active. However, r_y^m in this paper is attained by wireless power transfer, which is $r_y^m = \mathbb{E}_{\boldsymbol{x}}(\boldsymbol{x}^T\mathbf{g}_m^T\mathbf{g}_m\boldsymbol{x})$. Then, we have:

$$\lambda_{i,m} = \mathbb{E}_{\boldsymbol{x}}(\boldsymbol{x}^T\mathbf{g}_m^T\mathbf{g}_m\boldsymbol{x})\frac{\xi_{i,m}\beta^2(\frac{f_c}{4\pi})^{2\beta}}{d_{i,m}^{2\beta+2}N_0} \tag{14}$$

It is clearly observed that $\boldsymbol{x}$ is the beamforming strategy and $\boldsymbol{x}^T\mathbf{g}_m^T\mathbf{g}_m\boldsymbol{x}$ determines the localization accuracy directly in (12). Thus, the two phase propagations are integrated as a new FIM. For instance, $\lambda_{i,m} = \lambda_{m,i}$ for WCNs if both active nodes send the same signal powers. However, in our system, $\lambda_{i,m} \neq \lambda_{m,i}$ even if $\boldsymbol{x}$ contains the same waveforms for all the antennas. Because the wireless power propagation channels from antennas to the nodes are different.

D. Squared Position Error Bound

Although CRLB is the widely used localization performance indicator for unbiased estimation algorithms, a specified scalar value is preferred for quantify the localization accuracy. Generally, the mean square error (MSE) or root mean squared error (RMSE) are closely related to the trace of CRLB. In this case, SPEB which is the trace of CRLB is employed as the optimal performance metric [3]. For a single target node, we define SPEB as:

$$\mathcal{P}(\boldsymbol{p}_i) \triangleq \mathrm{tr}\{\mathbf{J}^{-1}(\boldsymbol{p}_i)\} \tag{15}$$

Then, for multiple target nodes, the SPEB is expressed as follows:

$$\mathcal{P}(\boldsymbol{\theta}) \triangleq \sum_{i=1}^{N_T} \mathrm{tr}\{\mathbf{J}^{-1}(\boldsymbol{p}_i)\} = \mathrm{tr}\{\mathbf{J}^{-1}(\boldsymbol{\theta})\} \tag{16}$$

In addition, using SPEB as the scalar value can derive a tighter bound during relaxing the following optimization problems.

IV. Beamforming Schemes for Full Connected Network

A. Localization Accuracy Optimization

It is clearly observed that the wireless power beam directly influence the localization performance. With the given FIM to indicate the SPEB, we formulate beamforming problems for WPCNs as the optimal cooperative localization problem.

Considering the sum of transmitter power is constrained, the minimum SPEB is to decide how to design the wireless power wave forms to achieve the minimum location estimation error:

$$\begin{aligned} (\mathbb{P}_1) : &\min_{\boldsymbol{x}} \mathcal{P}(\boldsymbol{\theta}) \\ &s.t. \ \ \mathbb{E}_{\boldsymbol{x}}(\boldsymbol{x}\boldsymbol{x}^T) \leq P_c \end{aligned} \tag{17}$$

where P_c is the sum power constraint. Here, we assume that all the nodes, including the anchors and the target nodes, can receive effective signals when the system is deployed. Thus, the minimum received energy constraint is ignored. It is clearly observed that $\mathbb{P}_1$ is complicated to expand and it is also a monotonically nonincreasing function of $\mathbf{J}(\boldsymbol{\theta})$. Then, we apply the following propositions to relax the objectives:

$$\mathbf{J}(\boldsymbol{\theta})=\begin{pmatrix}\mathbf{J}_A(\boldsymbol{p}_1)+\sum_{m\neq 1}\mathbf{C}_{1,m} & -\mathbf{C}_{1,2} & \cdots & -\mathbf{C}_{1,N_T}\\ -\mathbf{C}_{1,2} & \mathbf{J}_A(\boldsymbol{p}_2)+\sum_{m\neq 2}\mathbf{C}_{2,m}\cdots & & -\mathbf{C}_{2,N_T}\\ \vdots & \vdots & \ddots & \vdots\\ -\mathbf{C}_{1,N_T} & -\mathbf{C}_{2,N_T} & \cdots\mathbf{J}_A(\boldsymbol{p}_{N_T})+\sum_{m\neq N_T}\mathbf{C}_{N_T,m}\end{pmatrix}. \tag{12}$$

Proposition 2. *The SPEB satisfies that* $\mathcal{P}(\boldsymbol{\theta})\geq 4N_T^2\frac{1}{\mathrm{tr}\{\mathbf{J}(\boldsymbol{\theta})\}}$. *The* " $=$ " *holds if and only if* $\tau_1=\tau_2=\ldots=\tau_{2N_T}$, *where* $\tau_1,\tau_2,\ldots,\tau_{2N_T}$ *are the eigenvalues of* $\mathbf{J}(\boldsymbol{\theta})$.

Proof. *Refer to Appendix B for the detailed derivation.*

Using Proposition 2, $\mathbb{P}_1$ can be relaxed to the maximum $\mathrm{tr}\{\mathbf{J}(\boldsymbol{\theta})\}$ problem:

$$\begin{aligned}(\mathbb{P}_1^*):&\max_{\boldsymbol{x}}\mathrm{tr}\{\mathbf{J}(\boldsymbol{\theta})\}\\ &s.t.\ \ \mathbb{E}_{\boldsymbol{x}}(\boldsymbol{x}\boldsymbol{x}^T)\leq P_c\end{aligned} \tag{18}$$

where $\mathrm{tr}\{\mathbf{J}(\boldsymbol{\theta})\}$ is derived according to (56) in Appendix B:

$$\mathrm{tr}\{\mathbf{J}(\boldsymbol{\theta})\}=\boldsymbol{x}^T(\mathbf{G}_A^T\sum_{i=1}^{N_T}\boldsymbol{\Lambda}_i\mathbf{G}_A+\mathbf{G}_C^T(\sum_{i=1}^{N_T}\boldsymbol{\Gamma}_i+\boldsymbol{\Xi})\mathbf{G}_C)\boldsymbol{x} \tag{19}$$

and $\boldsymbol{\Lambda}_i$, $\boldsymbol{\Gamma}_i$ and $\boldsymbol{\Xi}$ are derived in (57), (60) and (58).

B. Close-form Solution

The above objective is a typical quadratically constrained quadratical programming (QCQP). One feasible solution is to use Lagrangian relaxation and Lagrangian multiplier method to approximate the optimal value. Here we define $\boldsymbol{\Psi}=\mathbf{G}_A^T\sum_{i=1}^{N_T}\boldsymbol{\Lambda}_i\mathbf{G}_A+\mathbf{G}_C^T(\sum_{i=1}^{N_T}\boldsymbol{\Gamma}_i+\boldsymbol{\Xi})\mathbf{G}_C$, and it is clear that $\boldsymbol{\Psi}$ is a positive defined matrix due to the nature of FIM. Then, we define the multiplier $\mu>0$, and construct the Lagrangian function of $\mathbb{P}_1^*$ as follows:

$$\mathcal{F}_1(\boldsymbol{x},\mu)=-\boldsymbol{x}^T\boldsymbol{\Psi}\boldsymbol{x}-\mu(P_c-\boldsymbol{x}^T\boldsymbol{x}) \tag{20}$$

where we convert the objective $\max_{\boldsymbol{x}}\mathrm{tr}\{\mathbf{J}(\boldsymbol{\theta})\}$ into $\min_{\boldsymbol{x}}-\mathrm{tr}\{\mathbf{J}(\boldsymbol{\theta})\}$. Then, the Karush-Kuhn-Tucker (KKT) conditions are attained:

$$\frac{\partial\mathcal{F}_1(\boldsymbol{x},\mu)}{\partial\boldsymbol{x}}=-\boldsymbol{\Psi}\boldsymbol{x}+\mu\boldsymbol{x}^T\boldsymbol{x}=0 \tag{21}$$

Since $\mu\neq 0$, we have:

$$\boldsymbol{\Psi}\boldsymbol{x}=\mu\boldsymbol{x}. \tag{22}$$

According to the definition of matrix eigenvalue, it is obvious that μ is one of the eigenvalues for matrix $\boldsymbol{\Psi}$, and $\boldsymbol{x}$ is the corresponding eigenvector. Since $\boldsymbol{\Psi}$ is a positive semi-definite Hermitian matrix, it can be eigen-decomposed to $\boldsymbol{\Psi}=\mathbf{Q}\boldsymbol{\Phi}\mathbf{Q}^T$, where $\mathbf{Q}$ is the unitary matrix and $\boldsymbol{\Phi}$ is a diagonal matrix of the eigenvalues of $\boldsymbol{\Psi}$. Then, define $\acute{\boldsymbol{x}}=\mathbf{Q}^T\boldsymbol{x}$, and $\varsigma_1,\ldots,\varsigma_K$ are the real and non-negative eigenvalues of $\boldsymbol{\Psi}$. Then, we have $\boldsymbol{x}^T\boldsymbol{\Psi}\boldsymbol{x}=\sum_k\varsigma_k|\acute{x}_k|^2$, where $\acute{\boldsymbol{x}}=(0,\ldots,0,\acute{x}_k,0,\ldots,0)$, and $|\acute{x}_k|^2=1$. In this case, the maximal $\boldsymbol{x}^T\boldsymbol{\Psi}\boldsymbol{x}$ is attained with $\varsigma_{max}=\arg\max\{\varsigma_1,\ldots,\varsigma_K\}$. Thus, the optimal solution $\boldsymbol{x}^{\mathrm{opt}}$ is proportional to the corresponding column of $\mathbf{Q}$. Considering the power constraint P_c, the optimal $\boldsymbol{x}^{\mathrm{opt}}=c\cdot\mathrm{maxeig}(\boldsymbol{\Psi})$, where c is an adapting co-efficient to make the sum of signal power approach P_c.

C. Energy Efficiency Optimization

The energy efficiency problem in cooperative localization of WPCN is to achieve the minimum Tx power of E-AP with given localization requirements constraints. The localization requirements mean that the estimation error of each node should not exceed a typical threshold, which is defined as ρ_{th}. Thus, the energy efficiency problem is expressed as:

$$\begin{aligned}(\mathbb{P}_2):&\min_{\boldsymbol{x}}\mathbb{E}_{\boldsymbol{x}}(\boldsymbol{x}\boldsymbol{x}^T)\\ &s.t.\ \ \mathcal{P}(\boldsymbol{\theta})\leq N_T\rho_{th}\end{aligned} \tag{23}$$

where the localization should satisfy the average localization requirements. Similar to $\mathbb{P}_1$, we can relax $\mathbb{P}_2$ according to Proposition 2:

$$\begin{aligned}(\mathbb{P}_2^*):&\min_{\boldsymbol{x}}\mathbb{E}_{\boldsymbol{x}}(\boldsymbol{x}\boldsymbol{x}^T)\\ &s.t.\ \boldsymbol{x}^T(\mathbf{G}_A^T\sum_{i=1}^{N_T}\boldsymbol{\Lambda}_i\mathbf{G}_A+\mathbf{G}_C^T(\sum_{i=1}^{N_T}\boldsymbol{\Gamma}_i+\boldsymbol{\Xi})\mathbf{G}_C)\boldsymbol{x}\geq\frac{4N_T}{\rho_{th}}\end{aligned} \tag{24}$$

However, $\mathbb{P}_2^*$ cannot provide a close form solution, since it may not be always convex. Thus, we employ the SDP to relax such problem. Firstly, let $\mathbf{X}=\boldsymbol{x}^T\boldsymbol{x}$ and it is obvious that $\mathrm{rank}(\mathbf{X})=1$. Consider $\boldsymbol{x}\boldsymbol{x}^T=\mathrm{tr}(\mathbf{X})$ and $\boldsymbol{x}^T\boldsymbol{\Omega}\boldsymbol{x}=\mathrm{tr}(\mathbf{Q}\mathbf{X})$, where $\boldsymbol{\Omega}$ indicate any symmetric matrix, then $\mathbb{P}_2^*$ is equivalent to:

$$\begin{aligned}(\widetilde{\mathbb{P}}_2^*):&\min_{\mathbf{X}}\mathrm{tr}(\mathbf{X})\\ &s.t.\ \mathrm{tr}((\mathbf{G}_A^T\sum_{i=1}^{N_T}\boldsymbol{\Lambda}_i\mathbf{G}_A+\mathbf{G}_C^T(\sum_{i=1}^{N_T}\boldsymbol{\Gamma}_i+\boldsymbol{\Xi})\mathbf{G}_C)\mathbf{X})\geq\frac{4N_T}{\rho_{th}}\\ &\quad\ \mathbf{X}\succeq\mathbf{0}\end{aligned} \tag{25}$$

which is a typical SDP problem and can be solved by many efficient tools, e.g., CVX. When $\mathbf{X}$ is attained, we have $\mathbf{X}=\lambda_0\mathbf{q}_0\mathbf{q}_0^T$, where λ_0 is the eigenvalue of rank one matrix and $\mathbf{q}_0$ is the corresponding eigenvector. Then, the feasible solution of $\boldsymbol{x}$ is $\boldsymbol{x}^*=\sqrt{\lambda_0}\mathbf{q}_0$.

D. Calibrations

Note that using Proposition 2 to solve $(\widetilde{\mathbb{P}}_2^*)$ can only meet a loose bound of the localization requirement, since several relaxations are employed. Thus, the localization requirement constraints are not met even if the optimal solutions are attained. However, such loose bound can be adapted into a tight bound by introducing a coefficient c_0 to $\frac{4N_T}{\rho_{th}}$, which means that we can set a value during the computation to force the relaxed constraints strictly approach the real localization requirements. Therefore, we employ a self-calibration method

and divide the SDP solutions into two steps. In the first step, we set $c_0 = 1$, and turn $(\widetilde{\mathbb{P}}_2^*)$ as follows:

$$\begin{aligned}(\widetilde{\mathbb{P}}_{2-c}^*) : &\min_{\mathbf{X}} \mathrm{tr}(\mathbf{X}) \\ &s.t.\ \mathrm{tr}((\mathbf{G}_A^T \sum_{i=1}^{N_T} \mathbf{\Lambda}_i \mathbf{G}_A + \mathbf{G}_C^T (\sum_{i=1}^{N_T} \mathbf{\Gamma}_i + \mathbf{\Xi}) \mathbf{G}_C)\mathbf{X}) \geq \frac{c_0}{\rho_{th} N_T} \\ &\mathbf{X} \geq \mathbf{0}\end{aligned} \tag{26}$$

where we change $\frac{4N_T}{\rho_{th}}$ into $\frac{c_0}{\rho_{th} N_T}$ in order to simplify the further calibration and approach the real localization requirements. When the optimal solution $\boldsymbol{x}^*$ is attained, we substitute $\boldsymbol{x}^*$ into (11). Then, we attain a real trace of FIM $\widetilde{\rho} = \mathbf{J}^{-1}(\boldsymbol{\theta}|\boldsymbol{x}^*)$ based on $\boldsymbol{x}^*$, and we set $c_0 = \frac{\widetilde{\rho}}{\rho_{th} N_T}$. The final optimal solution is attained when the SDP of $\mathbb{P}_{2-c}^*$ is executed again with new c_0, and the localization requirements are met as well.

V. Spatial Recursive Formulations for Single Target

A. Spatial Recursive Optimization

When the $N_T + 1$th node joins the network, the other nodes will send the ranging signals to help this node attain its initial location. However, the ranging signals for the other N_T node localizations are not exploited. Then, we define the whole estimated vector as $\boldsymbol{\theta}_s = [\mathbf{p}_{N_T+1}^T \ \mathbf{p}_1^T \ \mathbf{p}_2^T \ \cdots \ \mathbf{p}_{N_T}^T]^T = [\mathbf{p}_{N_T+1}^T \ \boldsymbol{\theta}^T]^T$. The FIM is formulated as (28) and using Shur complement, we have (29) on top of the next page where:

$$\begin{cases} \mathbf{C}_{N_T+1,i} = \mathbf{C}_{i,N_T+1} = (\lambda_{N_T+1,i} + \lambda_{i,N_T+1}) \mathbf{J}(\phi_{N_T+1,i}) \\ \mathbf{M}_{N_T+1} = [-\mathbf{C}_{N_T+1,1} \ -\mathbf{C}_{N_T+1,2} \ \cdots \ -\mathbf{C}_{N_T+1,N_T}] \end{cases} \tag{27}$$

and $\mathbf{I}_{N_T \times N_T}$ is the identical matrix with $N_T \times N_T$ dimensions, and $\otimes$ is the Kronecker product.

However, using such FIM of optimization will lead to higher order programming, which is too complicated to solve. Thus, we derive a new upper bound of $\mathbf{J}(\mathbf{p}_{N_T+1})$ by ignoring some parts of $\mathbf{J}(\mathbf{p}_{N_T+1})$, which is

$$\mathbf{J}_U(\mathbf{p}_{N_T+1}) = \mathbf{J}_A(\mathbf{p}_{N_T+1}) + \sum_{i \neq N_T+1} \mathbf{C}_{N_T+1,i} \tag{30}$$

Using the elementary algebra, we obtain the inequality:

$$\mathbf{J}(\boldsymbol{\theta}_s) \preceq \mathbf{J}_U(\boldsymbol{\theta}_s) \tag{31}$$

Then, we attain the lower bound $\mathcal{P}(\mathbf{p}_{N_T+1}) \geq \mathcal{P}_L(\mathbf{p}_{N_T+1}) = \mathrm{tr}(\mathbf{J}_U^{-1}(\mathbf{p}_{N_T+1}))$. Thus, we can use the minimum $\mathcal{P}_L(\mathbf{p}_{N_T+1})$ to indicate the lower bound of $\mathcal{P}(\mathbf{p}_{N_T+1})$. In this case, we just need to attain the maximum $\mathrm{tr}(\mathbf{J}_U(\mathbf{p}_{N_T+1}))$.

Using Proposition 2, the spatial recursive beamforming is formulated as:

$$\begin{aligned}(\mathbb{P}_3^*) : &\max_{\boldsymbol{x}} \mathrm{tr}\{\mathbf{J}_U(\mathbf{p}_{N_T+1})\} \\ &s.t. \quad \mathbb{E}_{\boldsymbol{x}}(\boldsymbol{x}\boldsymbol{x}^T) \leq P_c\end{aligned} \tag{32}$$

which is also QCQP. Similar to $\mathbb{P}_1^*$, $\mathrm{tr}\{\mathbf{J}_U(\mathbf{p}_{N_T+1})\}$ is a simplified form according to (19):

$$\mathrm{tr}\{\mathbf{J}_U(\mathbf{p}_{N_T+1})\} = \boldsymbol{x}^T (\mathbf{G}_A^T \mathbf{\Lambda}_{N_T+1} \mathbf{G}_A + \mathbf{G}_C^T (\sum_{i=1}^{N_T} \mathbf{\Gamma}_i) \mathbf{G}_C) \boldsymbol{x} \tag{33}$$

Similarly, we can construct KKT conditions just like (21), and use eigenvalue decomposition to attain the optimal vector $\boldsymbol{x}^*$.

B. Energy Efficiency Problem

For energy efficiency purpose, we still use $\mathbf{J}_U(\mathbf{p}_{N_T+1})$ to relax $\mathbf{J}(\mathbf{p}_{N_T+1})$. Although such relaxation is not tight, the computation overhead is efficiently reduced. Then, using Proposition 2, the objective is expressed as:

$$\begin{aligned}(\mathbb{P}_4^*) : &\min_{\boldsymbol{x}} \mathbb{E}_{\boldsymbol{x}}(\boldsymbol{x}\boldsymbol{x}^T) \\ &s.t. \quad \mathrm{tr}\{\mathbf{J}_U(\mathbf{p}_{N_T+1})\} \geq \frac{4}{\rho_{th}}\end{aligned} \tag{34}$$

Similar to $\mathbb{P}_2^*$, we employ $\mathbf{X} = \boldsymbol{x}^T \boldsymbol{x}$ to relax $\mathbb{P}_4^*$ and we attain the SDP formulations:

$$\begin{aligned}(\widetilde{\mathbb{P}}_4^*) : &\min_{\mathbf{X}} \mathrm{tr}(\mathbf{X}) \\ &s.t. \quad \mathrm{tr}\{\mathbf{J}_U(\mathbf{p}_{N_T+1})\} \geq \frac{4}{\rho_{th}} \\ &\mathbf{X} \geq \mathbf{0}\end{aligned} \tag{35}$$

which can also be solved by CVX.

C. Calibration

Note that $\widetilde{\mathbb{P}}_4^*$ still attains a loose bound of the localization requirements. In this case, a two-step calibration method which is similar to $\mathbb{P}_2^*$ is developed. In this calibration, we also employ a coefficient c_0 to adapt the constraints. The first step is to set $c_0 = 1$ and we obtain:

$$\begin{aligned}(\widetilde{\mathbb{P}}_{4-c}^*) : &\min_{\mathbf{X}} \mathrm{tr}(\mathbf{X}) \\ &s.t. \quad \mathrm{tr}\{\mathbf{J}_U(\mathbf{p}_{N_T+1})\} \geq \frac{c_0}{\rho_{th}} \\ &\mathbf{X} \geq \mathbf{0}\end{aligned} \tag{36}$$

Then, the initial optimal solution $\boldsymbol{x}^*$ is attained. In the second step, we use $\boldsymbol{x}^*$ to derive the actual trace of $\mathbf{J}(\mathbf{p}_{N_T+1})$, and compute $\widetilde{\rho} = \mathbf{J}^{-1}(\mathbf{p}_{N_T+1})$. Then, we still set $c_0 = \frac{\widetilde{\rho}}{\rho_{th}}$, and use SDP to attain the final solution of $\widetilde{\mathbb{P}}_{4-c}^*$.

VI. Channel Uncertainty

In the real applications, the channel states are time-varying and interfered by the noise. Thus, the beamforming schemes should also consider the channel uncertainty problem. Then, the optimizations are re-formulated accordingly and the impact of the uncertainty should be analyzed.

Considering that the k-th antenna sends the pilot signal with power q_k to node n, node n will estimate the channel state and feedback to the E-AP. The minimum mean square error (MMSE) of g_{kn} is denoted by $\tilde{g}_{kn}$, and the estimation error is $e_{kn} \triangleq \tilde{g}_{kn} - g_{kn}$, which is a random variables with zero mean and variance [46]:

$$\sigma_{kn}^2 = \frac{\beta_{kn}}{1 + \beta_{kn} L q_k / \sigma^2} \tag{37}$$

where β_{kn} is the path loss from antenna k to node n, L indicates the symbol length and σ^2 is the background noise variance. Considering the estimation error is i.i.d, it is easily attained $||g_{kn}||^2 = ||\tilde{g}_{kn}||^2 + \sigma_{kn}^2$, and $\mathbb{E}(g_{kn} g_{km}) = \tilde{g}_{kn} \tilde{g}_{km}$.

$$\mathbf{J}(\boldsymbol{\theta}_s)=\begin{pmatrix}\mathbf{J}_A(\mathbf{p}_{N_T+1})+\sum_{i\neq N_T+1}\mathbf{C}_{N_T+1,i} & -\mathbf{C}_{N_T+1,1} & \dots & -\mathbf{C}_{N_T+1,N_T}\\ -\mathbf{C}_{1,N_T+1} & \mathbf{J}_A(\mathbf{p}_1)+\sum_{i\neq 1}\mathbf{C}_{1,i}\dots & & -\mathbf{C}_{1,N_T}\\ \vdots & \vdots & \ddots & \vdots\\ -\mathbf{C}_{N_T,N_T+1} & -\mathbf{C}_{N_T,1} & \dots\mathbf{J}_A(\mathbf{p}_{N_T})+\sum_{i\neq N_T}\mathbf{C}_{N_T,i}\end{pmatrix} \tag{28}$$

$$\mathbf{J}(\mathbf{p}_{N_T+1})=\mathbf{J}_A(\mathbf{p}_{N_T+1})+\sum_{i\neq N_T+1}\mathbf{C}_{N_T+1,i}-\mathbf{M}_{N_T+1}(\mathbf{J}(\boldsymbol{\theta})+\mathbf{I}_{N_T\times N_T}\otimes\mathbf{M}_{N_T+1})^{-1}\mathbf{M}_{N_T+1}^T \tag{29}$$

Then, we update the received power for node n in (2) with the channel uncertainty model:

$$\tilde{r}_y^n=\boldsymbol{x}^T\begin{pmatrix}||\tilde{g}_{1n}||^2+\sigma_{1n}^2 & \tilde{g}_{1n}\tilde{g}_{2n} & \dots & \tilde{g}_{1n}\tilde{g}_{Kn}\\ \tilde{g}_{2n}\tilde{g}_{1n} & ||\tilde{g}_{2n}||^2+\sigma_{2n}^2 & \dots & \tilde{g}_{2n}\tilde{g}_{Kn}\\ \vdots & \vdots & \ddots & \vdots\\ \tilde{g}_{Kn}\tilde{g}_{1n} & \tilde{g}_{Kn}\tilde{g}_{2n} & \dots & ||\tilde{g}_{Kn}||^2+\sigma_{Kn}^2\end{pmatrix}\boldsymbol{x} \tag{38}$$

Statistically, $\tilde{g}_{kn}\tilde{g}_{km}$ is equivalent to $g_{kn}g_{km}$. In this case, the FIM and the localization estimation accuracy does not only rely on the channel state but also depends on the estimation error of the wireless power propagation channel. And the estimation error mainly influences the diagonal elements in $\tilde{r}_y^n$. To simplify the analysis, we mainly use the pilot signal-to-noise-ratio (SNR) as the main parameter to indicate the channel uncertainty.

VII. Simulation

The proposed schemes are evaluated by extensive simulations. In the simulations, we assume that all nodes including 10 anchors and several targets are randomly deployed in a $500\times 500\ \mathrm{m}^2$ playing field. The antenna array of E-AP can be deployed in the center of the playing field or randomly deployed throughout the whole playing field. The signal carrier frequency is 2.4 GHz and the maximum allowed transmitted power of E-AP is 30 dBm (1 W). In addition, the received power of each node for communications and harvesting energy is -90 dBm, and the power of the background noise is -130 dBm. We assume a free space propagation model of the wireless power transfer channel, and the NLOS ranging is not considered in FIM calculation [3].

We use SPEB to indicate the localization accuracy and use the total transmitted power of E-AP as the energy efficiency metric. Since our schemes are to relax the trace of FIM and employ quadratic programming or SDP to solve the optimization problems, our schemes are indicated as Tr-QP or Tr-SDP. The proposed schemes are compared with equally combining scheme (EC), which allocates the transmitted power equally and the same wave form on each antenna, and SDP based power allocation schemes in [14], [39], [40].

To transfer the power allocation from WCN to WPCN, we consider the signals from E-AP is orthogonal $\mathbb{E}(\sum_{k\neq l}x_kx_l)=0$. Then, $r_y^n=\mathbb{E}(\sum_{k=1}^K||g_{kn}||^2||x_k||^2)$. Define the channel power gain vector for the node n $\bar{\mathbf{g}}_n=[\mathbb{E}(||g_{1n}||^2),\ \mathbb{E}(||g_{1n}||^2),\dots,\ \mathbb{E}(||g_{Kn}||^2)]^T$, and define $\mathbf{r}_x=[r_x^1,\ r_x^2,\dots,\ r_x^K]$ as the transmitter power vector of $\boldsymbol{x}$, where $r_x^k=\mathbb{E}(||x_k||^2),\ k\in\{1,\ 2,\ \dots,\ K\}$. Then, we have:

$$r_y^n=\bar{\mathbf{g}}_n^T\mathbf{r}_x \tag{39}$$

It is clearly observed that r_y^n is determined by the power allocation of $\mathbf{r}_x$. Then, we re-formulate $\mathbf{J}(\boldsymbol{\theta}|\mathbf{r}_x)$ and substitute it into $\mathbf{J}(\boldsymbol{\theta})$ in the problem formulations. And we also employ $\mathbf{r}_x$ to indicate $\mathbb{E}_{\boldsymbol{x}}(\boldsymbol{x}\boldsymbol{x}^T)$. In this case, the energy beamforming problem is converted into a power allocation problem. For SDP solutions, one optional method is to employ an auxiliary covariance matrix $\mathbf{Z}$ [39], which satisfies that $\mathbf{J}^{-1}(\boldsymbol{\theta}|\mathbf{r}_x)\succeq\mathbf{Z}^{-1}$. Using linear matrix inequality (LMI), we have:

$$\begin{pmatrix}\mathbf{J}(\boldsymbol{\theta}|\mathbf{r}_x) & \mathbf{I}\\ \mathbf{I} & \mathbf{Z}\end{pmatrix}\succeq\mathbf{0} \tag{40}$$

where $\mathbf{I}$ is the identical matrix with the same dimension of $\mathbf{J}(\boldsymbol{\theta}|\mathbf{r}_x)$ and $\mathbf{Z}$. Then, we can use $\mathbf{Z}$ either as the objective or localization requirement, which is a typical SDP problem. However, such method is over relaxed and far from the actual FIM value especially in the cooperative localization framework. Thus, we still employ the trace of $\mathbf{J}(\boldsymbol{\theta}|\mathbf{r}_x)$ and re-formulate the objectives, which are still SDP problems.

A. Full Connected Network Evaluation

Firstly, the beamforming strategies for cooperative localization of WPCN are evaluated in a sequential way, in which the nodes harvest the energy from beamformed microwaves and exchange signals during each time slots, and then fuse the previous FIM to derive the current SPEBs. The averaged SPEBs of all the schemes are illustrated in Fig. 2. It is clearly observed that the estimation error of Tr-QP is much lower than the other two. Compare with SDP, Tr-QP can effectively use the spatial correlations to increase the performance. While the results of SDP only allocate the major power on one antenna, which ignores the benefits of the correlated channels. In this case, SDP is even slightly worse than EC. However, with the previous information, the SPEBs of three schemes gradually converge to a quite low value.

Then, we increase the cooperative nodes from 10 to 100. As illustrated in Fig. 3, the SPEBs of all three schemes drop down with more nodes participating in the localization. The Tr-QP outperforms other schemes even with only 10 cooperative nodes, and the related SPEB only decreases a limited value with more cooperative nodes.

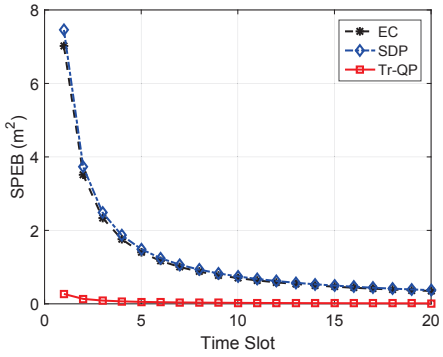

Fig. 2. Sequential Evaluation of SPEB. The SPEB contains the previous FIM.

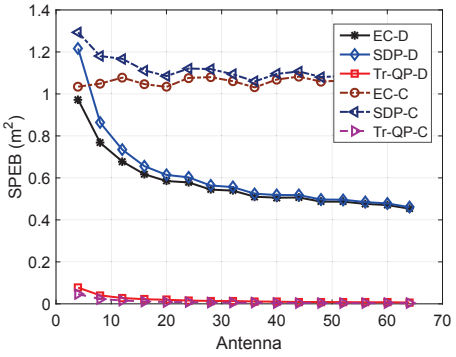

Fig. 4. The SPEBs with different antennas of E-APs. In this simulation, we consider both centralized and distributed antennas.

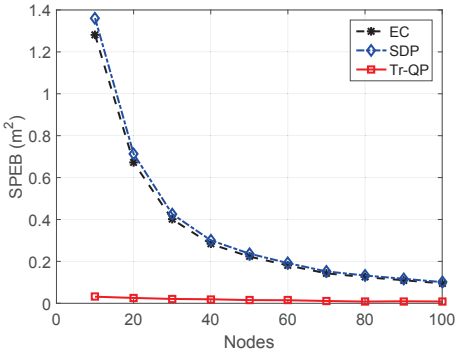

Fig. 3. Cooperative node evaluation. We increase the nodes to check whether it will benefit the localization performance.

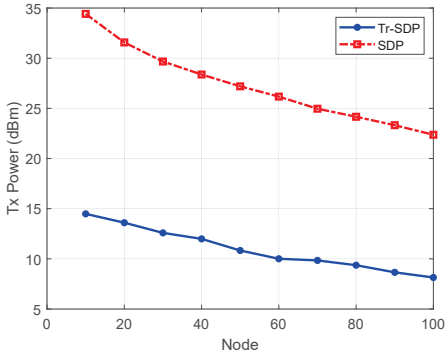

(a) Tx power consumption with different number of cooperative nodes.

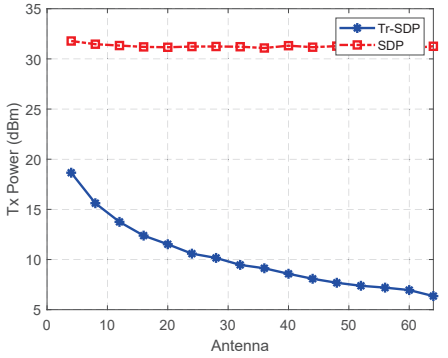

(b) Tx power consumption with different number of antennas.

Fig. 5. Energy efficiency evaluation for full connected network.

Next, we adapt the antennas of E-AP to examine the impacts for cooperative localizations. In this simulation, we also evaluate the impacts of both centralized and distributed antennas of E-APs. For centralized antennas, we assume there is only one E-AP with a Tx antenna array that is deployed in the center of the playing field. For distributed antennas, we assume multiple E-APs randomly deployed in the whole playing field and each E-AP contains only one antenna. We adapt the number of antennas from 4 to 64. The SPEBs of three schemes in both cases are depicted in Fig. 4. For EC and SDP schemes, the distributed antennas outperform the centralized antennas. In addition, more antennas can benefit both schemes. However, the SPEBs of Tr-QP in both cases are quite similar, and the centralized antenna array is slightly better than the distributed antennas. Increasing the number of antennas reduces the SPEBs of Tr-QP but not too much since the initial values are below 0.1 with only 4 antennas.

Further, we evaluate the power consumptions of our proposed energy efficiency schemes. We compare our SDP based scheme, which is named by Tr-SDP, with the SDP based power allocation scheme. The average SPEB requirement is 1 m^2. The cooperative node number and the antenna number are also adapted to evaluate the performance, in which the SPEB is used to indicate localization accuracy and the total Tx power (dBm) is the energy efficiency metric. The results are depicted in Fig. 5. As illustrated in Fig. 5(a) and Fig. 5(b), the total Tx power of Tr-SDP is lower than SDP. With the participation of more nodes and antennas, the power consumptions are gradually reduced.

B. Spatial Recursive Evaluation

In the spatial recursive simulation, the nodes join the network one by one, and we apply the proposed scheme to attain the optimal SPEB of the new node. The number of anchors is 10. The power constraint is 30 dBm for optimal localization problems, and we employ the spatial recursive form of Tr-QP to solve $\mathbb{P}_3^*$. We also compare our scheme with SDP and EC for a single node. As indicated in Fig. 6, the

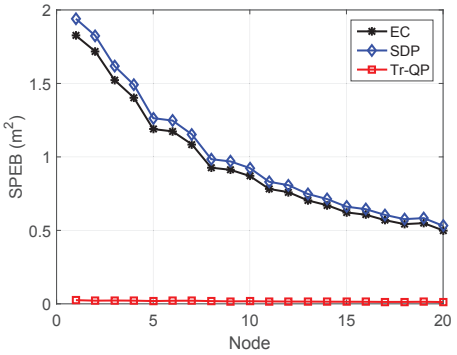

Fig. 6. The SPEBs for single node evaluation.

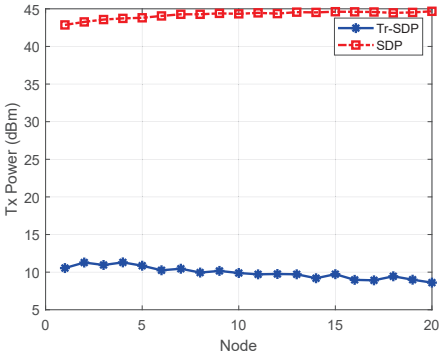

Fig. 7. The Tx power consumptions for single node evaluation.

SPEBs of SDP and EC are decreasing when more nodes join the network. However, the Tr-QP maintains a low value which is below 0.2 when the network only contains one node, and such value is kept even with more nodes joining the network, which outperforms the other two schemes.

For energy efficiency optimization, the localization requirement constraint is 1 m^2, and we apply Tr-SDP to solve $\widetilde{\mathbb{P}}_4^*$. We also compare our scheme with SDP schemes, and the power consumptions are illustrated in Fig. 7, in which Tr-SDP consumes less power than SDP and such value even drops with more nodes.

C. Channel Uncertainty Evaluation

Finally, we introduce the channel uncertainty model into the simulations to evaluate the impacts. We still use 10 anchors and 20 nodes, and the simulation parameters are the same as mentioned before. For channel estimations, the accuracy mainly relies on the transmitted pilot power and the noise. Therefore, we employ the pilot SNR to indicate the channel estimation parameter. Then, we adapt the SNR from -30 dB to 20 dB, and both Tr-QP for optimal localization and Tr-SDP for energy efficiency are analyzed. In Fig. 8, the SPEB of Tr-QP with lower SNR is higher than the Tr-QP with ideal channel information, which demonstrates the degrading localization accuracy due to the inaccurate channel estimation. When the SNR is increased, the SEPB with channel uncertainty is gradually reduced and approaching the ideal case.

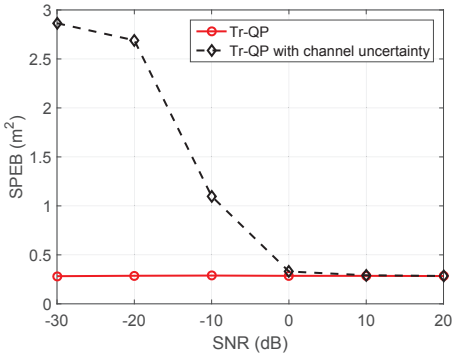

Fig. 8. The SPEB evaluation with channel uncertainty.

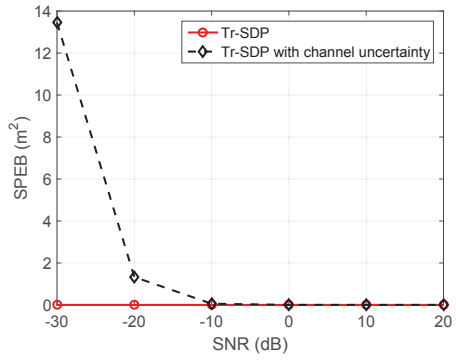

(a) SPEB results.

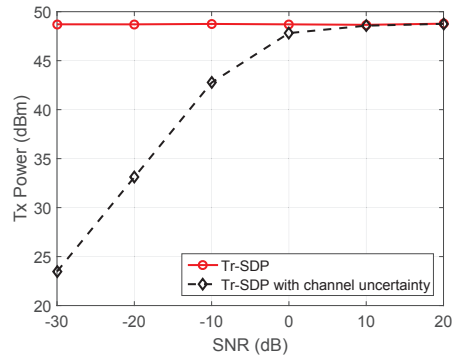

(b) Tx power consumptions.

Fig. 9. Energy efficiency evaluation with channel uncertainty.

Such impacts also lead to the unreliable energy consumptions, as illustrated in Fig. 9(a). The SPEB of Tr-SDP with lower SNR is much higher than the ideal channel case, which indicates that the localization requirements are not guaranteed and SPEBs are wrongly derived. And the Tx power is reduced with higher SPEBs. However, such power reduction is mainly caused by the unreliable SPEB due to the channel uncertainty, because the localization requirement constraints are not bounded any more during the SDP calculations. In this case, the system consumes less power compared with ideal case, because it considers the required localization accuracy is already achieved.

VIII. Conclusion

In this paper, we analyze the fundamental limits of the cooperative localization in WPCNs. We formulate the cooperative FIM and propose the beamforming schemes to solve the localization accuracy and energy efficiency optimization problems. In addition, the spatial recursive form and related beamforming schemes are also investigated. The simulations demonstrate that our schemes outperform the power allocation based SDP methods and equally combining power scheme. With more nodes and more antennas of E-AP participating, the localization accuracy is increased. We also observe that the channel uncertainty affect the localization accuracy and consume more power to achieve the localization requirements.

Appendix A
FIM for Cooperative Localization in WPCN

According to (8), the log likelihood function for θ consists of two parts:

$$\ln f(\boldsymbol{z}|\boldsymbol{\theta}) = \ln f(\boldsymbol{z}_A|\boldsymbol{\theta}) + \ln f(\boldsymbol{z}_C|\boldsymbol{\theta}) \tag{41}$$

For the first part $\ln f(\boldsymbol{z}_A|\boldsymbol{\theta})$, the score function is (42), where $\ln f(\boldsymbol{z}_i^A|\boldsymbol{p}_i) = \sum_{j=1}^{N_A} \ln f(z_{j,i}|\boldsymbol{p}_i)$ is the sum log likelihood for $\boldsymbol{p}_i$ based on the observations from anchors.

Due to the independence of the received signals for different target nodes, $\frac{\partial \ln f(\boldsymbol{z}_m^A|\boldsymbol{p}_i)}{\partial \boldsymbol{p}_i} = 0, m \neq i$, then we have a diagonal matrix:

$$\mathbf{U}_A(\boldsymbol{\theta}) = \begin{pmatrix} \frac{\partial \ln f(\boldsymbol{z}_1^A|\boldsymbol{p}_1)}{\partial \boldsymbol{p}_1} & & \\ & \ddots & \\ & & \frac{\partial \ln f(\boldsymbol{z}_{N_T}^A|\boldsymbol{p}_{N_T})}{\partial \boldsymbol{p}_{N_T}} \end{pmatrix} \tag{43}$$

For each $\frac{\partial \ln f(z_{j,i}|\boldsymbol{p}_i)}{\partial \boldsymbol{p}_i}$, we decompose it according to the chain rule:

$$\frac{\partial \ln f(z_{j,i}|\boldsymbol{p}_i)}{\partial \boldsymbol{p}_i} = y_j \cdot \frac{\partial h_{j,i}(d_{j,i})}{\partial d_{j,i}} \cdot \mathbf{q}_{j,i} \tag{44}$$

where $\mathbf{q}_{j,i} = [\cos\phi_{j,i} \ \ \sin\phi_{j,i}]^T$ with $\phi_{j,i} = \arctan\frac{p_i^X - p_j^X}{p_i^Y - p_j^Y}$. Here, we consider a flat fading channel, in which the path loss follows:

$$r_z^{j,i} = r_y^j \left(\frac{f_c}{4\pi d_{j,i}}\right)^{2\beta} \xi_{j,i} \tag{45}$$

where $r_z^{j,i}$ indicates the received signal power from anchor j to target i, and f_c represents the central frequency of the signal. If the signal noise follows zero-mean Gaussian distribution with the power N_0, we have:

$$\mathbb{E}\left(\frac{\partial \ln f(z_{j,i}|\boldsymbol{p}_i)}{\partial \boldsymbol{p}_i} \frac{\partial \ln f(z_{j,i}|\boldsymbol{p}_i)}{\partial \boldsymbol{p}_i}^T\right) = r_y^j \frac{\xi_{j,i}\beta^2 (\frac{f_c}{4\pi})^{2\beta}}{d_{j,i}^{2\beta+2} N_0} \mathbf{J}(\phi_{j,i}) \tag{46}$$

where $\mathbf{J}(\phi_{j,i}) = \mathbf{q}_{j,i}\mathbf{q}_{j,i}^T$ and r_y^j is attained according to (2). Then, we employ $\lambda_{j,i}$ to indicate the equivalent ranging coefficient (ERC):

$$\lambda_{j,i} = \mathbb{E}_{\boldsymbol{x}}(\boldsymbol{x}^T \mathbf{g}_j^T \mathbf{g}_j \boldsymbol{x}) \frac{\xi_{j,i}\beta^2 (\frac{f_c}{4\pi})^{2\beta}}{d_{j,i}^{2\beta+2} N_0} \tag{47}$$

and we obtain $\mathbf{J}_A(\boldsymbol{p}_i)$:

$$\mathbf{J}_A(\boldsymbol{p}_i) = \mathbb{E}\left(\frac{\partial \ln f(\boldsymbol{z}_i^A|\boldsymbol{p}_i)}{\partial \boldsymbol{p}_i} \frac{\partial \ln f(\boldsymbol{z}_i^A|\boldsymbol{p}_i)}{\partial \boldsymbol{p}_i}^T\right) = \sum_{j=1}^{N_T} \lambda_{j,i} \mathbf{J}(\phi_{j,i}) \tag{48}$$

Then, $\mathbf{J}_A(\boldsymbol{\theta}) = \mathbf{diag}(\mathbf{J}_A(\boldsymbol{p}_1), \ldots, \mathbf{J}_A(\boldsymbol{p}_{N_T}))$ is attained.

Similarly, we have $\mathbf{U}_C(\boldsymbol{\theta}) = \nabla_{\boldsymbol{\theta}} \ln f(\boldsymbol{z}_C|\boldsymbol{\theta})$ and attain (49) on top of the next page, where $\ln f(\boldsymbol{z}_i^C|\boldsymbol{p}_i) = \sum_{m=1}^{N_T} \ln f(z_{m,i}|\boldsymbol{p}_i)$ is the sum log likelihood for $\boldsymbol{p}_i$ based on the observations sending from all the target nodes to target i. In addition, $\frac{\partial \ln f(\boldsymbol{z}_m^C|\boldsymbol{p}_i)}{\partial \boldsymbol{p}_i} = \frac{\partial \ln f(z_{i,m}|\boldsymbol{p}_i)}{\partial \boldsymbol{p}_i}, m \neq i$. Then, $\mathbf{U}_C(\boldsymbol{\theta})$ is simplified as right side form in (49).

For $\frac{\partial \ln f(\boldsymbol{z}_i^C|\boldsymbol{p}_i)}{\partial \boldsymbol{p}_i}$, we have similar results to $\ln f(\boldsymbol{z}_i^A|\boldsymbol{p}_i)$, in which each $\frac{\partial \ln f(z_{m,i}|\boldsymbol{p}_i)}{\partial \boldsymbol{p}_i}, m \neq i$:

$$\frac{\partial \ln f(z_{m,i}|\boldsymbol{p}_i)}{\partial \boldsymbol{p}_i} = y_m \cdot \frac{\partial h_{m,i}(d_{m,i})}{\partial d_{m,i}} \cdot \mathbf{q}_{m,i}. \tag{50}$$

Similarly, $\frac{\partial \ln f(z_{i,m}|\boldsymbol{p}_i)}{\partial \boldsymbol{p}_i}$ is:

$$\frac{\partial \ln f(z_{i,m}|\boldsymbol{p}_i)}{\partial \boldsymbol{p}_i} = y_i \cdot \frac{\partial h_{i,m}(d_{i,m})}{\partial d_{i,m}} \cdot \mathbf{q}_{i,m} \tag{51}$$

where $\mathbf{q}_{i,m} = -\mathbf{q}_{m,i}$. Then, substitute $\frac{\partial \ln f(z_{i,m}|\boldsymbol{p}_i)}{\partial \boldsymbol{p}_i}$ and $\frac{\partial \ln f(\boldsymbol{z}_i^C|\boldsymbol{p}_i)}{\partial \boldsymbol{p}_i}$ into $\mathbf{J}_C(\boldsymbol{\theta}) = \mathbb{E}(\mathbf{U}_C(\boldsymbol{\theta})\mathbf{U}_C^T(\boldsymbol{\theta}))$, we have:

$$\mathbf{J}_C(\boldsymbol{\theta}) = \begin{pmatrix} \sum_{m\neq 1} \mathbf{C}_{1,m} & -\mathbf{C}_{1,2} & \cdots & -\mathbf{C}_{1,N_T} \\ -\mathbf{C}_{1,2} & \sum_{m\neq 2} \mathbf{C}_{2,m} & \cdots & -\mathbf{C}_{2,N_T} \\ \vdots & \vdots & \ddots & \vdots \\ -\mathbf{C}_{1,N_T} & -\mathbf{C}_{2,N_T} & \cdots & \sum_{m\neq N_T} \mathbf{C}_{N_T,m} \end{pmatrix}. \tag{52}$$

where $\mathbf{C}_{m,i} = (\lambda_{i,m} + \lambda_{m,i})\mathbf{J}(\phi_{m,i}); i \neq m \in \mathcal{N}_T$, and $\lambda_{i,m}$ is:

$$\lambda_{m,i} = \mathbb{E}_{\boldsymbol{x}}(\boldsymbol{x}^T \mathbf{g}_m^T \mathbf{g}_m \boldsymbol{x}) \frac{\xi_{m,i}\beta^2 (\frac{f_c}{4\pi})^{2\beta}}{d_{m,i}^{2\beta+2} N_0} \tag{53}$$

Then, $\mathbf{J}(\boldsymbol{\theta}) = \mathbf{J}_A(\boldsymbol{\theta}) + \mathbf{J}_C(\boldsymbol{\theta})$.

Appendix B
Proof and Derivation of Traces of $\mathbf{J}(\boldsymbol{\theta})$ and $\mathbf{J}^{-1}(\boldsymbol{\theta})$

We decompose $\mathbf{J}(\boldsymbol{\theta})$ as follows:

$$\mathbf{J}(\boldsymbol{\theta}) = \mathbf{U}_\psi \begin{pmatrix} \tau_1 & & & \\ & \tau_2 & & \\ & & \ddots & \\ & & & \tau_{2N_T} \end{pmatrix} \mathbf{U}_\psi^T \tag{54}$$

where $\mathbf{U}_\psi$ is the eigenvector matrix and $\tau_1, \ldots, \tau_{N_T}$ are the corresponding eigenvalues. Then, $\mathrm{tr}\{\mathbf{J}(\boldsymbol{\theta})\} = \sum_{i=1}^{2N_T} \tau_i$ and $\mathcal{P}(\boldsymbol{\theta}) = \sum_{i=1}^{2N_T} \frac{1}{\tau_i}$. Consider each eigenvalue is positive in FIM, we attain the following formulation according to [47]:

$$\frac{2N_T}{\sum_{i=1}^{2N_T} \frac{1}{\tau_i}} \leq \frac{1}{2N_T} \sum_{i=1}^{2N_T} \tau_i \tag{55}$$

Then, we obtain $\mathcal{P}(\boldsymbol{\theta}) \geq 4N_T^2 \frac{1}{\mathrm{tr}\{\mathbf{J}(\boldsymbol{\theta})\}}$.

$$\mathbf{U}_A(\boldsymbol{\theta}) = \nabla_{\boldsymbol{\theta}} \ln f(\boldsymbol{z}_A|\boldsymbol{\theta}) = \begin{pmatrix} \frac{\partial \ln f(\boldsymbol{z}_1^A|\boldsymbol{p}_1)}{\partial \boldsymbol{p}_1} & \frac{\partial \ln f(\boldsymbol{z}_2^A|\boldsymbol{p}_1)}{\partial \boldsymbol{p}_1} & \cdots & \frac{\partial \ln f(\boldsymbol{z}_{N_T}^A|\boldsymbol{p}_1)}{\partial \boldsymbol{p}_1} \\ \frac{\partial \ln f(\boldsymbol{z}_1^A|\boldsymbol{p}_2)}{\partial \boldsymbol{p}_2} & \frac{\partial \ln f(\boldsymbol{z}_2^A|\boldsymbol{p}_2)}{\partial \boldsymbol{p}_2} & \cdots & \frac{\partial \ln f(\boldsymbol{z}_{N_T}^A|\boldsymbol{p}_2)}{\partial \boldsymbol{p}_2} \\ \vdots & \vdots & \ddots & \vdots \\ \frac{\partial \ln f(\boldsymbol{z}_1^A|\boldsymbol{p}_{N_T})}{\partial \boldsymbol{p}_{N_T}} & \frac{\partial \ln f(\boldsymbol{z}_2^A|\boldsymbol{p}_{N_T})}{\partial \boldsymbol{p}_{N_T}} & \cdots & \frac{\partial \ln f(\boldsymbol{z}_{N_T}^A|\boldsymbol{p}_{N_T})}{\partial \boldsymbol{p}_{N_T}} \end{pmatrix} \tag{42}$$

$$\mathbf{U}_C(\boldsymbol{\theta}) = \begin{pmatrix} \frac{\partial \ln f(\boldsymbol{z}_1^C|\boldsymbol{p}_1)}{\partial \boldsymbol{p}_1} & \frac{\partial \ln f(\boldsymbol{z}_2^C|\boldsymbol{p}_1)}{\partial \boldsymbol{p}_1} & \cdots & \frac{\partial \ln f(\boldsymbol{z}_{N_T}^C|\boldsymbol{p}_1)}{\partial \boldsymbol{p}_1} \\ \frac{\partial \ln f(\boldsymbol{z}_1^C|\boldsymbol{p}_2)}{\partial \boldsymbol{p}_2} & \frac{\partial \ln f(\boldsymbol{z}_2^C|\boldsymbol{p}_2)}{\partial \boldsymbol{p}_2} & \cdots & \frac{\partial \ln f(\boldsymbol{z}_{N_T}^C|\boldsymbol{p}_2)}{\partial \boldsymbol{p}_2} \\ \vdots & \vdots & \ddots & \vdots \\ \frac{\partial \ln f(\boldsymbol{z}_1^C|\boldsymbol{p}_{N_T})}{\partial \boldsymbol{p}_{N_T}} & \frac{\partial \ln f(\boldsymbol{z}_2^C|\boldsymbol{p}_{N_T})}{\partial \boldsymbol{p}_{N_T}} & \cdots & \frac{\partial \ln f(\boldsymbol{z}_{N_T}^C|\boldsymbol{p}_{N_T})}{\partial \boldsymbol{p}_{N_T}} \end{pmatrix} = \begin{pmatrix} \frac{\partial \ln f(\boldsymbol{z}_1^C|\boldsymbol{p}_1)}{\partial \boldsymbol{p}_1} & \frac{\partial \ln f(z_{1,2}|\boldsymbol{p}_1)}{\partial \boldsymbol{p}_1} & \cdots & \frac{\partial \ln f(z_{1,N_T}|\boldsymbol{p}_1)}{\partial \boldsymbol{p}_1} \\ \frac{\partial \ln f(z_{2,1}|\boldsymbol{p}_2)}{\partial \boldsymbol{p}_2} & \frac{\partial \ln f(\boldsymbol{z}_2^C|\boldsymbol{p}_2)}{\partial \boldsymbol{p}_2} & \cdots & \frac{\partial \ln f(z_{2,N_T}|\boldsymbol{p}_2)}{\partial \boldsymbol{p}_2} \\ \vdots & \vdots & \ddots & \vdots \\ \frac{\partial \ln f(z_{N_T,1}|\boldsymbol{p}_{N_T})}{\partial \boldsymbol{p}_{N_T}} & \frac{\partial \ln f(z_{N_T,2}|\boldsymbol{p}_{N_T})}{\partial \boldsymbol{p}_{N_T}} & \cdots & \frac{\partial \ln f(\boldsymbol{z}_{N_T}^C|\boldsymbol{p}_{N_T})}{\partial \boldsymbol{p}_{N_T}} \end{pmatrix} \tag{49}$$

For $\mathbf{J}(\boldsymbol{\theta})$:

$$\begin{aligned} \mathrm{tr}\{\mathbf{J}(\boldsymbol{\theta})\} &= \mathrm{tr}(\sum_{i=1}^{N_T} \mathbf{J}_A(\boldsymbol{p}_i) + \sum_{i=1}^{N_T}\sum_{m\neq i}^{N_T} \mathbf{C}_{m,i}) \\ &= \sum_{i=1}^{N_T}\sum_{j=1}^{N_A} \lambda_{j,i} + \sum_{i=1}^{N_T}\sum_{m\neq i}^{N_T} (\lambda_{i,m} + \lambda_{m,i}) \\ &= \mathbf{D}_A + \mathbf{D}_C \end{aligned} \tag{56}$$

Substitute (47) into $\mathbf{D}_A$, we attain:

$$\mathbf{D}_A = \boldsymbol{x}^T \mathbf{G}_A^T \sum_{i=1}^{N_T} \boldsymbol{\Lambda}_i \mathbf{G}_A \boldsymbol{x} \tag{57}$$

where $\boldsymbol{\Lambda}_i = \mathrm{diag}(\frac{\xi_{1,i}\beta^2(\frac{f_c}{4\pi})^{2\beta}}{d_{1,i}^{2\beta+2}N_0}, \ldots, \frac{\xi_{N_A,i}\beta^2(\frac{f_c}{4\pi})^{2\beta}}{d_{N_A,i}^{2\beta+2}N_0})$. Then, we substitute (53) into $\mathbf{D}_C$ and divide $\mathbf{D}_C = \sum_{i=1}^{N_T}\sum_{m\neq i}^{N_T} \lambda_{i,m} + \sum_{i=1}^{N_T}\sum_{m\neq i}^{N_T} \lambda_{m,i}$ to attain (59) where $\boldsymbol{\Gamma}_i$ is formulated as (60) and $\boldsymbol{\Xi}$ is expressed as:

$$\boldsymbol{\Xi} = \mathrm{diag}(\sum_{m\neq 1}^{N_T} \frac{\xi_{1,m}\beta^2(\frac{f_c}{4\pi})^{2\beta}}{d_{1,m}^{2\beta+2}N_0}, \ldots, \sum_{m\neq N_T}^{N_T} \frac{\xi_{N_T,m}\beta^2(\frac{f_c}{4\pi})^{2\beta}}{d_{N_T,m}^{2\beta+2}N_0}) \tag{58}$$

REFERENCES

[1] J. Huang, Y. Zhou, Z. Ning, and H. Gharavi, "Wireless Power Transfer and Energy Harvesting: Current Status and Future Prospects," *IEEE Wireless Communications*, vol. 26, no. 4, pp. 163–169, 2019.

[2] R. Bansal, "The Future of Wireless Charging," *IEEE Antennas and Propagation Magazine*, vol. 51, no. 2, pp. 153–153, 2009.

[3] Y. Shen and M. Z. Win, "Fundamental Limits of Wideband Localization‡ Part I: A General Framework," *IEEE Transactions on Information Theory*, vol. 56, no. 10, pp. 4956–4980, Oct 2010.

[4] K. W. Choi, L. Ginting, A. A. Aziz, D. Setiawan, J. H. Park, S. I. Hwang, D. S. Kang, M. Y. Chung, and D. I. Kim, "Toward Realization of Long-Range Wireless-Powered Sensor Networks," *IEEE Wireless Communications*, vol. 26, no. 4, pp. 184–192, 2019.

[5] P. Biswas, T. C. Lian, T. C. Wang, and Y. Ye, "Semidefinite Programming based Algorithms for Sensor Network Localization," *ACM Transactions on Sensor Networks*, vol. 2, no. 2, pp. 188–220, 2006.

[6] G. Yang, C. K. Ho, R. Zhang, and Y. L. Guan, "Throughput Optimization for Massive MIMO Systems Powered by Wireless Energy Transfer," *IEEE Journal on Selected Areas in Communications*, vol. 33, no. 8, pp. 1640–1650, Aug 2015.

[7] F. Tan, T. Lv, and P. Huang, "Global Energy Efficiency Optimization for Wireless-Powered Massive MIMO Aided Multiway AF Relay Networks," *IEEE Transactions on Signal Processing*, vol. 66, no. 9, pp. 2384–2398, May 2018.

[8] Y. Kim, T. J. Lee, and D. I. Kim, "Joint Information and Power Transfer in SWIPT-Enabled CRFID Networks," *IEEE Wireless Communications Letters*, vol. 7, no. 2, pp. 186–189, 2018.

[9] G. Loubet, A. Takacs, and D. Dragomirescu, "Implementation of a Battery-Free Wireless Sensor for Cyber-Physical Systems Dedicated to Structural Health Monitoring Applications," *IEEE Access*, vol. 7, pp. 24 679–24 690, 2019.

[10] W. Feng, N. Zhao, S. Ao, J. Tang, X. Zhang, Y. Fu, D. K. C. So, and K. K. Wong, "Joint 3D Trajectory Design and Time Allocation for UAV-Enabled Wireless Power Transfer Networks," *IEEE Transactions on Vehicular Technology*, vol. 69, no. 9, pp. 9265–9278, 2020.

[11] J. Rezazadeh, R. Subramanian, K. Sandrasegaran, X. Kong, M. Moradi, and F. Khodamoradi, "Novel iBeacon Placement for Indoor Positioning in IoT," *IEEE Sensors Journal*, vol. 18, no. 24, pp. 10 240–10 247, 2018.

[12] W. Dai, Y. Shen, and M. Z. Win, "Distributed Power Allocation for Cooperative Wireless Network Localization," *IEEE Journal on Selected Areas in Communications*, vol. 33, no. 1, pp. 28–40, Jan 2015.

[13] Y. Shen, W. Dai, and M. Z. Win, "Power Optimization for Network Localization," *IEEE/ACM Transactions on Networking*, vol. 22, no. 4, pp. 1337–1350, Aug 2014.

[14] W. W. Li, Y. Shen, Y. J. Zhang, and M. Z. Win, "Robust Power Allocation for Energy-Efficient Location-Aware Networks," *IEEE/ACM Transactions on Networking*, vol. 21, no. 6, pp. 1918–1930, Dec 2013.

[15] H. Ju and R. Zhang, "Throughput Maximization in Wireless Powered Communication Networks," *IEEE Transactions on Wireless Communications*, vol. 13, no. 1, pp. 418–428, January 2014.

[16] Y. L. Che, L. Duan, and R. Zhang, "Spatial Throughput Maximization of Wireless Powered Communication Networks," *IEEE Journal on Selected Areas in Communications*, vol. 33, no. 8, pp. 1534–1548, Aug 2015.

[17] N. K. D. Venkategowda, H. Lee, and I. Lee, "Joint Transceiver Designs for MSE Minimization in MIMO Wireless Powered Sensor Networks," *IEEE Transactions on Wireless Communications*, vol. 17, no. 8, pp. 5120–5131, 2018.

[18] Z. Zhou, M. Peng, and Z. Zhao, "Joint Data-Energy Beamforming and Traffic Offloading in Cloud Radio Access Networks With Energy Harvesting-Aided D2D Communications," *IEEE Transactions on Wireless Communications*, vol. 17, no. 12, pp. 8094–8107, 2018.

[19] H. Wang, J. Wang, G. Ding, and Z. Han, "D2D Communications Underlaying Wireless Powered Communication Networks," *IEEE Transactions on Vehicular Technology*, vol. 67, no. 8, pp. 7872–7876, 2018.

[20] K. Liang, L. Zhao, G. Zheng, and H. Chen, "Non-Uniform Deployment of Power Beacons in Wireless Powered Communication Networks," *IEEE Transactions on Wireless Communications*, vol. 18, no. 3, pp. 1887–1899, 2019.

[21] T. Ha, J. Kim, and J. Chung, "HE-MAC: Harvest-Then-Transmit Based Modified EDCF MAC Protocol for Wireless Powered Sensor Networks," *IEEE Transactions on Wireless Communications*, vol. 17, no. 1, pp. 3–16, 2018.

$$\mathbf{D}_C = \boldsymbol{x}^T \mathbf{G}_C^T (\sum_{i=1}^{N_T} \boldsymbol{\Gamma}_i) \mathbf{G}_C \boldsymbol{x} + \boldsymbol{x}^T \mathbf{G}_C^T \boldsymbol{\Xi} \mathbf{G}_C \boldsymbol{x} = \boldsymbol{x}^T \mathbf{G}_C^T (\sum_{i=1}^{N_T} \boldsymbol{\Gamma}_i + \boldsymbol{\Xi}) \mathbf{G}_C \boldsymbol{x} \tag{59}$$

$$\boldsymbol{\Gamma}_i = \mathrm{diag}(\frac{\xi_{1,i}\beta^2(\frac{f_c}{4\pi})^{2\beta}}{d_{1,i}^{2\beta+2}N_0}, \ldots, \frac{\xi_{i-1,i}\beta^2(\frac{f_c}{4\pi})^{2\beta}}{d_{i-1,i}^{2\beta+2}N_0}, 0, \frac{\xi_{i+1,i}\beta^2(\frac{f_c}{4\pi})^{2\beta}}{d_{i+1,i}^{2\beta+2}N_0}, \ldots, \frac{\xi_{N_T,i}\beta^2(\frac{f_c}{4\pi})^{2\beta}}{d_{N_T,i}^{2\beta+2}N_0}) \tag{60}$$

[22] J. Chen, L. Zhang, Y. Liang, X. Kang, and R. Zhang, "Resource Allocation for Wireless-Powered IoT Networks With Short Packet Communication," *IEEE Transactions on Wireless Communications*, vol. 18, no. 2, pp. 1447–1461, 2019.

[23] Y. Qian, J. Yan, H. Guan, J. Li, X. Zhou, S. Guo, and D. N. K. Jayakody, "Design of Hybrid Wireless and Power Line Sensor Networks With Dual-Interface Relay in IoT," *IEEE Internet of Things Journal*, vol. 6, no. 1, pp. 239–249, 2019.

[24] T. V. Nguyen, T. Do, V. N. Q. Bao, D. B. d. Costa, and B. An, "On the Performance of Multihop Cognitive Wireless Powered D2D Communications in WSNs," *IEEE Transactions on Vehicular Technology*, vol. 69, no. 3, pp. 2684–2699, 2020.

[25] W. Wang, J. Tang, N. Zhao, X. Liu, X. Y. Zhang, Y. Chen, and Y. Qian, "Joint Precoding Optimization for Secure SWIPT in UAV-Aided NOMA Networks," *IEEE Transactions on Communications*, vol. 68, no. 8, pp. 5028–5040, 2020.

[26] M. R. Basheer and S. Jagannathan, "Localization of RFID Tags using Stochastic Tunneling," *IEEE transactions on mobile computing*, vol. 12, no. 6, pp. 1225–1235, 2012.

[27] R. Vauche, E. Bergeret, J. Gaubert, S. Bourdel, O. Fourquin, and N. Dehaese, "A Remotely UHF Powered UWB Transmitter for High Precision Localization of RFID Tag," in *2011 IEEE International Conference on Ultra-Wideband (ICUWB)*. IEEE, 2011, pp. 494–498.

[28] P. Pannuto, B. Kempke, and P. Dutta, "Slocalization: Sub-uW Ultra Wideband Backscatter Localization," in *2018 17th ACM/IEEE International Conference on Information Processing in Sensor Networks (IPSN)*. IEEE, 2018, pp. 242–253.

[29] M. Fantuzzi, D. Masotti, and A. Costanzo, "Rectenna Array with RF-Uncoupled Closely-spaced Monopoles for Autonomous Localization," in *2018 48th European Microwave Conference (EuMC)*. IEEE, 2018, pp. 765–768.

[30] ——, "A Multilayer Compact-size UWB-UHF Antenna System for Novel RFID Applications," in *2015 European Microwave Conference (EuMC)*. IEEE, 2015, pp. 255–258.

[31] ——, "A Novel Integrated UWB–UHF One-port Antenna for Localization and Energy Harvesting," *IEEE Transactions on Antennas and Propagation*, vol. 63, no. 9, pp. 3839–3848, 2015.

[32] A. El Assaf, S. Zaidi, S. Affes, and N. Kandil, "Efficient Node Localization in Energy-Harvesting Wireless Sensor Networks," in *2015 IEEE International Conference on Ubiquitous Wireless Broadband (ICUWB)*. IEEE, 2015, pp. 1–7.

[33] Z. Chang, X. Wu, W. Wang, and G. Chen, "Localization in Wireless Rechargeable Sensor Networks using Mobile Directional Charger," in *2015 IEEE Global Communications Conference (GLOBECOM)*. IEEE, 2015, pp. 1–6.

[34] D. Belo, D. C. Ribeiro, P. Pinho, and N. B. Carvalho, "A Selective, Tracking, and Power Adaptive Far-Field Wireless Power Transfer System," *IEEE Transactions on Microwave Theory and Techniques*, vol. 67, no. 9, pp. 3856–3866, 2019.

[35] A. A. Aziz, L. Ginting, D. Setiawan, J. H. Park, N. M. Tran, G. Y. Yeon, D. I. Kim, and K. W. Choi, "Battery-Less Location Tracking for Internet of Things: Simultaneous Wireless Power Transfer and Positioning," *IEEE Internet of Things Journal*, vol. 6, no. 5, pp. 9147–9164, 2019.

[36] Y. Zhao, X. Li, Y. Ji, and C. Xu, "Wireless Power-Driven Positioning System: Fundamental Analysis and Resource Allocation," *IEEE Internet of Things Journal*, vol. 6, no. 6, pp. 10 421–10 430, 2019.

[37] M. Z. Win, R. M. Buehrer, G. Chrisikos, A. Conti, and H. V. Poor, "Foundations and Trends in Localization Technologies: Part I," *Proceedings of the IEEE*, vol. 106, no. 6, pp. 1019–1021, June 2018.

[38] Y. Shen, H. Wymeersch, and M. Z. Win, "Fundamental Limits of Wideband Localizationł Part II: Cooperative Networks," *IEEE Transactions on Information Theory*, vol. 56, no. 10, pp. 4981–5000, 2010.

[39] W. Dai, Y. Shen, and M. Z. Win, "Energy-Efficient Network Navigation Algorithms," *IEEE Journal on Selected Areas in Communications*, vol. 33, no. 7, pp. 1418–1430, July 2015.

[40] T. Zhang, A. F. Molisch, Y. Shen, Q. Zhang, H. Feng, and M. Z. Win, "Joint Power and Bandwidth Allocation in Wireless Cooperative Localization Networks," *IEEE Transactions on Wireless Communications*, vol. 15, no. 10, pp. 6527–6540, 2016.

[41] J. Chen, W. Dai, Y. Shen, V. K. N. Lau, and M. Z. Win, "Resource Management Games for Distributed Network Localization," *IEEE Journal on Selected Areas in Communications*, vol. 35, no. 2, pp. 317–329, 2017.

[42] B. Peng, G. Seco-Granados, E. Steinmetz, M. Frohle, and H. Wymeersch, "Decentralized Scheduling for Cooperative Localization With Deep Reinforcement Learning," *IEEE Transactions on Vehicular Technology*, vol. 68, no. 5, pp. 4295–4305, 2019.

[43] S. Safavi, U. A. Khan, S. Kar, and J. M. F. Moura, "Distributed Localization: A Linear Theory," *Proceedings of the IEEE*, vol. 106, no. 7, pp. 1204–1223, 2018.

[44] T. V. Nguyen, Y. Jeong, H. Shin, and M. Z. Win, "Least Square Cooperative Localization," *IEEE Transactions on Vehicular Technology*, vol. 64, no. 4, pp. 1318–1330, 2015.

[45] R. M. Vaghefi and R. M. Buehrer, "Cooperative Localization in NLOS Environments Using Semidefinite Programming," *IEEE Communications Letters*, vol. 19, no. 8, pp. 1382–1385, 2015.

[46] S. M. Kay, *Fundamentals of Statistical Signal Processing: Estimation Theory*. Prentice Hall PTR, 1993.

[47] L. Rabinowitz, "Mathematical Statistics and Data Analysis," *Technometrics*, vol. 31, no. 3, pp. 390–391, 1989.

Yubin Zhao received his B.S. and M.S. in 2007 and 2010 respectively from Beijing University of Posts and Telecommunications (BUPT), Beijing, China. He received his Ph.D degree in computer science in 2014 from Freie Universität Berlin (FU Berlin), Berlin, Germany. He is currently an Associate Professor in Center for Cloud Computing, Shenzhen Institutes of Advanced Technology, Chinese Academy of Sciences, Shenzhen, China, since 2014. He serves as the guest editor and reviewer for several journals. He also received outstanding research award in CICCAT 2019. His current research interest includes wireless power transfer, indoor localization and target tracking.

Xiaofan Li received her B.S. degree and Ph.D degree from Beijing University of Posts and Telecommunication in 2007 and 2012. From 2010 to 2011, she studied in University of Washington as an exchanged Ph.D student. She joined the State Radio Monitoring Center and Testing Center (SRTC) from 2012 and was transferred to SRTC Shenzhen Lab from 2013. She is currently an associate professor in the School of Intelligent Systems Science and Engineering, Jinan University, Zhuhai, China. Her research interests include interference analysis among different radio systems, testing and evaluation methods for innovative radio technologies, cooperative communication, cognitive radio, internet of things, radio management strategy, etc.

Huaming Wu received the B.E. and M.S. degrees from Harbin Institute of Technology, China in 2009 and 2011, respectively, both in electrical engineering. He received the Ph.D. degree with the highest honor in computer science at Freie Universitt Berlin, Germany in 2015. He is currently an associate professor in the Center for Applied Mathematics, Tianjin University, China. His research interests include model-based evaluation, wireless and mobile network systems, mobile cloud computing and deep learning.

Cheng-Zhong Xu is the Dean of Faculty of Science and Technology, University of Macau, a Chair Professor of Computer and Information Science and the Interim Director of Institute of Collaborative Innovation. He also holds a courtesy position as the Director of the Center for Cloud Computing in Shenzhen Institutes of Advanced Technology (SIAT), Chinese Academy of Sciences. He was a Professor of Electrical and Computer Engineering at Wayne State University and the Director of Advanced Computing and Digital Engineering of SIAT. Dr. Xu's main research interests lie in parallel and distributed computing and cloud computing, in particular, with an emphasis on resource management for system's performance, reliability, availability, power efficiency, and security, and in big data and data-driven intelligence applications. The systems of particular interest include distributed systems and the Internet, servers and cloud datacenters, scalable parallel computers, and wireless embedded devices and mobile edge systems. He published two research monographs and more than 250 papers in journals and conference proceedings, including over 50 in IEEE/ACM transactions; his publications received more than 9000 citations with an H-index of 47. He was a Best Paper Nominee or Awardee of the 2013 IEEE High Performance Computer Architecture (HPCA), the 2013 ACM High Performance Distributed Computing (HPDC), IEEE Cluster2015, ICPP2015, GPC2018, and UIC2018. He also received more than 100 patents or PCT patents and spun off a business Shenzhen Baidou Applied Technology with dedication to location-based services and technologies. Dr. Xu received the most prestigious "President's Awards for Excellence in Teaching" of Wayne State University in 2002. He serves or served on a number of journal editorial boards, including IEEE Transactions on Computers (TC), IEEE Transactions on Cloud Computing (TCC), IEEE Transactions on Parallel and Distributed Systems (TPDS), Journal of Parallel and Distributed Computing (JPDC), Science China: Information Science and ZTE Communication. Dr. Xu has been the Chair of IEEE Technical Committee on Distributed Processing (TCDP) since 2015. He obtained BSc and MSc degrees from Nanjing University in 1986 and 1989 respectively, and a PhD degree from the University of Hong Kong in 1993, all in Computer Science and Engineering.